Impact of physical changes in mushroom on variation in moisture sorption

Journal of Food Engineering

Hu, Lina; Bi, Jinfeng; Jin, Xin; van der Sman, Ruud

https://doi.org/10.1016/j.jfoodeng.2023.111506

Journal of Food Engineering 351 (2023) 111506

Contents lists available at ScienceDirect

Journal of Food Engineering

journal homepage: www.elsevier.com/locate/jfoodeng

Impact of physical changes in mushroom on variation in moisture sorption

Lina Hu [a,b], Jinfeng Bi [a,*], Xin Jin [a,**], Ruud van der Sman [b,c]

[a] Institute of Food Science and Technology, Chinese Academy of Agricultural Sciences (CAAS), Key Laboratory of Agro-Products Processing, Ministry of Agriculture and Rural Affairs, Beijing 100193, China
[b] Food Process Engineering, Agrotechnology and Food Sciences Group, Wageningen University & Research, Bornse Weilanden 9, 6708 WG Wageningen, the Netherlands
[c] Food & Biobased Research, Wageningen University & Research, Bornse Weilanden 9, 6708WG, Wageningen, the Netherlands

ARTICLE INFO

Keywords:
Moisture sorption isotherms
Mushrooms
Viscoelasticity
Model

ABSTRACT

In this work, physical changes such as protein denaturation, cell membrane integrity, and the viscoelastic relaxation of mushrooms, as induced by drying treatments, were investigated as possible causes of the variation in moisture sorption isotherms (MSIs) and hysteresis. Our investigations involved both experimental and theoretical evaluation of MSIs. Via analysis with the Flory-Huggins (FH) theory, we concluded that 1) the protein denaturation does not significantly affect moisture sorption and hysteresis, and 2) cell membrane integrity only influences on the moisture sorption/water holding capacity at high relative humidity. Additional experiments show that mushrooms exhibit viscoelastic properties, which are temperature and moisture-dependent. As dynamic vapor sorption (DVS) experiments show signs of viscoelastic relaxation, we consider the latter to be the likely determining factor affecting the variations in MSI and hysteresis. The Flory-Rehner theory follows that one needs to include elastic stress into the driving force of drying. For viscoelastic media, a separate model, like the generalized Maxwell model, should describe the stress evolution linked to a drying model.

1. Introduction

Moisture sorption isotherms (MSIs) should ideally illustrate the equilibrium amount of water held by the food solids as a function of relative humidity at a constant temperature or equivalently as a function of water activity. Consequently, it can be used for the modeling and possible optimization of food drying procedures, as the water activity is related to the driving force for drying, i.e. the gradient in the chemical potential of water (Jin et al., 2014). However, many MSIs measurements conducted by food scientists via a single cycle of the sorption-desorption process do not exhibit equilibrium conditions, as evidenced by the existence of hysteresis (Burnett et al., 2006; Caurie, 2007). Hence, a good knowledge of the physical causes of the deviation of MSIs from equilibrium is essential (Dupas-Langlet et al., 2016).

Hysteresis has been given much attention in the field of wood drying. Several studies reported that during the multiple humid-dry cycles, the wood underwent a relaxation of internal mechanical stresses. The partial relaxation of stress results in wood samples, with different pretreatments, to exhibit similar hysteresis when exposed to the second and third cycles. The different hysteresis values during the first sorption-desorption cycle is attributed to the different amounts of mechanical stress build up during the various drying pretreatments (Hill et al., 2012). Therefore, we assume that MSIs obtained after multiple sorption-desorption measurements would better reflect the equilibrium moisture sorption properties of samples, as a consequence of the relaxation of the internal stress.

When exploring the causes rendering the differences in moisture sorption isotherms of different samples, researchers tend to attribute these to the changes in 1) hygroscopic properties induced by protein denaturation (Paudel et al., 2015; van der Sman, 2012); 2) microstructure properties, such as loss of cell membrane integrity (Lee and Lee, 2008; Pedro et al., 2010), or 3) mechanical properties like viscoelasticity (Fredriksson and Thybring, 2018; Hill et al., 2012; Patera et al., 2016; Salmén and Larsson, 2018). However, a detailed mechanistic interpretation of these factors on moisture sorption behaviour during multi-cycle dynamic vapor sorption (DVS) measurements, is still lacking.

In this work, we conducted dual cycle sorption-desorption DVS measurements on powdered dried *shiitake* mushroom samples obtained from different drying methods. Furthermore, we investigated the above mentioned factors affecting MSIs during the dual sorption-desorption

* Corresponding author.
** Corresponding author.
E-mail addresses: lina.hu@wur.nl (L. Hu), bjfcaas@126.com (J. Bi), jinxin@caas.cn (X. Jin), ruud.vandersman@wur.nl (R. van der Sman).

https://doi.org/10.1016/j.jfoodeng.2023.111506
Received 13 June 2022; Received in revised form 14 January 2023; Accepted 14 March 2023
Available online 15 March 2023

cycle. The effect of protein denaturation on MSIs is illustrated via the comparison of experiments with theoretical predictions based on the Flory-Huggins theory (Jin et al., 2014; Paudel et al., 2015; van der Sman, 2012). The cell membrane integrity of mushroom samples was identified by transmission electron microscopy (TEM). Subsequently, its effect on the MSIs of mushrooms is investigated by comparing the experimental data and the predicted MSIs calculated via the Flory-Huggins (FH) theory, while assuming cell wall and vacuole being a phase-separated system (Jin et al., 2014). We argue that overshoots observed in DVS experiments indicate the effect of stress relaxation and studied the viscoelastic properties of mushrooms via compression and stress relaxation tests on cylindrical mushroom samples with different moisture contents. Finally, we assume that the effect of stress relaxation can be explained by theory, where Flory-Rehner theory is coupled to a generalized Maxwell model, describing the viscoelastic property of the food material.

2. Material and methods

2.1. Materials preparation

Fresh *shiitake* mushrooms were used in this study and were purchased from a mushroom farm in Beijing (China). After cutting off the stem and cleaning with tap water, mushrooms were divided into three batches on average. One batch of mushrooms was dried with a freeze dryer (abbreviated as FD) (Alpila-aplus 4Lplus, Christ Co. Ltd., Osterode am Harz, Germany) under the same conditions as described in our previous study (Hu et al., 2021); the other two batches underwent hot air drying at 35 °C, 80 °C (abbreviated as HA35, HA80) with a hot air drier (DHG-9123 A, Shanghai Jinghong Experiment Facility Co., Ltd., Shanghai, China) with an air velocity of 1.2 m/s.

2.2. Measurement of moisture sorption isotherms on powdered dried mushrooms

Powdered dried mushroom samples (or dried mushroom powder) were obtained with a DFT-200 high-speed pulverizer (Linda, Wenling, China). The pulverization process lasted for 10 s, twice. The powder samples with relatively homogeneous particles were obtained after passing through 40 mesh sieves. Isotherms of powder samples weighing 22 mg ± 0.05 mg were determined at 25 °C with a dynamic vapor sorption analyzer (DVS) (Surface Measurement Systems Ltd., London, UK) equipped with a Cahn microbalance. Note that the powder samples were compacted on the specimen disc so that the structure of the pile of powder could be similar. Measurements were started by drying for 24 h at 0% RH, after which the RH was increased with 10% increments up to 90% RH, and then lowered again to 0% RH with 10% increments. This cycle of sorption/desorption was performed twice. A steady state was assumed when the weight change was less than 0.0005 min^{-1} over a window of 30 min. Isotherms were determined in duplicate.

2.3. Compression and stress relaxation test on cylindrical mushroom samples

Cylindrical mushroom samples were obtained from the cap of fresh mushrooms with a cylindrical steel tube cutter. The dimension of the fresh cylindrical samples was 10 mm ± 0.05 mm (diameter) × 10 mm ± 0.05 mm (height). These samples were dried to different moisture contents (Mc) at around 70%, 50%, 30%, and 10% (wet basis, w. b.) at 35 °C and 80 °C, respectively. Subsequently, compression stress relaxation tests were performed by TA. HD Plus Texture Analyzer (Stable Micro Systems, UK) with an AACC 36 mm cylinder probe with radius (P/36 R) and Exponent 5.1.2.0 software, similar to (Myhan et al., 2015). The speed of the loading during compression was 1 mm/s. In the relaxation phase, the sample was held at constant strain (30% of the initial sample height) for 60 s. We performed ten test replications on mushrooms obtained from different drying treatments.

2.4. Transmission electron microscopy (TEM)

The cellular structure of fresh mushroom and powdered dried mushroom samples was observed with a Hitachi H-7500 TEM (Hitachi, Tokyo, Japan) according to the method of (Hayat, 2012). The samples were treated as described in our previous work (Qiu et al., 2021). Each piece was imaged at least six times. Here, the fresh mushroom is used as the reference showing the state of the intact cell membrane.

2.5. Statistical analysis

The values in tables were presented by the means ± standard deviation. Statistical analysis was performed with SPSS software (Version 18.0, SPSS, Inc., Chicago, IL, USA), using analysis of variance (ANOVA) and Tukey test. Significant differences (at the $p < 0.05$ level) were expressed with small letters a-f.

3. Model description

3.1. Moisture sorption model

In the moisture sorption model, we take into account the impact of the cell membrane integrity of mushrooms on MSI. We view the mushroom powder with intact cell membranes as a phase-separated system, similar to our previous study (Jin et al., 2014). All solutes, such as sugars and ions, are located in the vacuole, which is considered a single-phase (Phase 1). On the other hand, all the biopolymers as proteins and fibers from the cytoplasm and cell wall, are assumed to be located in another phase (Phase 2). These phases are separated by the cell membrane (of the vacuole), whose permeability allows water to diffuse between the two phases. We assume local equilibrium between the two phases, leading to the partitioning of water over the two phases, such that the water activities of the two phases are equal. Therefore, the water activity of mushrooms with intact cell membranes follows:

$$a_{w,phase\ 1} = a_{w,phase\ 2} \quad (1)$$

But when the cell membrane is disrupted, the solutes from the vacuole can mix with the cell wall and cytoplasm, and hence we take the mushroom tissue as a single, homogeneous phase, with all compounds fully mixed.

The main compounds composing *shiitake* mushroom are listed in Table 1, with composition obtained from (Buwjoom et al., 2004; Carneiro et al., 2013; Julita Reguła, 2007; Reis et al., 2012). We display the averaged values from these data sources and list which phase they are located in (Phase 1: vacuole or Phase 2: cell wall/cytoplasm). We note that in all data sources, protein content is determined with a nitrogen-to-protein conversion factor of 4.38, which is required for the correction of nitrogen-containing chitin. The main ionic compound is potassium phosphate (KH_2PO_4) in mushrooms (Iiyama et al., 1996), which is considered that only 50% of the phosphate is soluble.

Table 1
Fraction of components in dry matter of shiitake mushrooms.

Component Location Content	Mannitol	Trehalose	Fiber	Protein	Ash (KH_2PO_4)
Phase1	✓	✓			✓
Phase2			✓	✓	
	0.307 ± 0.16	0.033 ± 0.016	0.375 ± 0.13	0.17 ± 0.11	0.0335 ± 0.007

Values are expressed as mean ± standard deviation.

For a solution with both neutral and charged solutes, the chemical potential of water can be computed simply by adding the contributions of the involved solutes (van der Sman, 2012):

$$\Delta\mu_{tot} = \Delta\mu_{mix} + \Delta\mu_{ion} \tag{2}$$

$\Delta\mu_{mix}$ is the contribution of neutral solutes, and $\Delta\mu_{ionic}$ is the contribution of ions. In terms of water activity, the contributions to the water activity can be multiplied as:

$$\mathbf{a}_{\mathrm{w,tot}} = \mathbf{a}_{\mathrm{w,mix}} * \mathbf{a}_{\mathrm{w,ion}} \tag{3}$$

The contribution of neutral solutes, $\mathbf{a}_{\mathrm{w,mix}}$, follows the Flory- Huggins (FH) theory. The free volume contribution to moisture sorption is zero, as the glass transition temperature of fresh *shiitake* mushrooms is already lower than the room temperature (Zhao et al., 2016). The contribution of ions (ash) $\mathbf{a}_{\mathrm{w,ion}}$ is described by the Pitzer equation. In the cell wall/cytoplasm phase (Phase 2), ions are absent, and FH theory can be used to compute the water activity of the water/biopolymer mixture.

For the phase-separated system, the water activities are as follows:

$$a_{w,phase\ 1} = \mathbf{a}_{\mathrm{w,mix\_polymer}} \tag{4}$$

$$a_{w,phase\ 2} = \mathbf{a}_{\mathrm{w,mix\_sugar}} * \mathbf{a}_{\mathrm{w,ion}} \tag{5}$$

According to the local equilibrium between the two phases, the volume fraction of water $\phi_{w,phase\ 1}, \phi_{w,phase\ 2}$ are adjusted, such that equal water activities are achieved under the constraint of a constant total amount of water. For this partitioning of water, we have used the minimization procedure present in the Scipy toolbox of Python.

Flory Huggins theory for $a_{w,mix}$.

Based on Flory Huggins theory (Jin et al., 2014; Paudel et al., 2015; van der Sman, 2012), the water activity $a_{w,mix}$ is:

$$ln\ a_{w,mix}(\phi_w, \chi_{eff}, N_{eff}) = ln(\phi_w) + \left(1 - \frac{1}{N_{eff}}\right)(1 - \phi_w) + \chi_{eff}(1 - \phi_w)^2 \tag{6}$$

in which ϕ_w is the volume fraction of water, which is the volume ratio of water and the sum of water and sugar, χ_{eff} is the effective interaction parameter, N_{eff} is the effective ratio of the molar volume of water versus solutes. The effective ratio of the molar volume of water versus that of the solutes (N_{eff}) is:

$$\frac{1}{N_{eff}} = \frac{\sum_i \frac{\phi_i}{N_i}}{\sum_i \phi_i} \tag{7}$$

ϕ_i is the volume fraction occupied by component i , N_i is the ratio of molar volumes of water and solute. For high molecular weight polymers like fiber and proteins, N_i could be 0.

χ_{eff} is the effective interaction parameter between components and water, which is given as:

$$\chi_{eff} = \frac{\sum_i \phi_i \chi_{iw}}{\sum_i \phi_i} \tag{8}$$

Here, χ_{iw} is the interaction parameter between component i and water, and ϕ_i is the volume fraction of component i. For trehalose and mannitol in mushrooms, the interaction parameters with water are constant with values of 0.5 and 0.37, respectively (van der Sman and Mauer, 2019). For polymers (fibers and protein), the interaction parameter is composition-dependent, which is as follows:

$$\chi_{iw} = \chi_{iw,0} + \left(\chi_{iw,1} - \chi_{iw,0}\right) * \left(1 - \tilde{\phi}_{w,eff}\right)^2 \tag{9}$$

in which $\chi_{iw,0}$ equals 0.5, and holds universally for all bipolymers, and $\chi_{iw,1}$ is the interaction parameter with the dry polymers i, which is specific for each biopolymer. $\chi_{iw,1}$ is constant at 0.8 for fibers. For proteins $\chi_{iw,1}$ is temperature dependent due to its denaturation. Over a relatively large temperature range, it changes from 0.8 to 1.4, following a logistic (sigmoid) function (Paudel et al., 2015; van der Sman, 2012):

$$\chi_{pw\ ,\ 1}(T) = \chi_{p1,0} + \frac{\chi_{p1,\infty} - \chi_{p1,0}}{1 + a * exp(b * (T - T_e))} \tag{10}$$

in which $\chi_{p1,0} = \mathbf{0.8}$ and $\chi_{p1,\infty} = \mathbf{1.4}$ are the values attained by $\chi_{iw,1}$ when the proteins are in their native state and fully denatured states, respectively. T is the processing temperature. T_e, the mid-point of the sigmoid curve, equals 350 K, which can be viewed as the protein denaturation temperature of *shiitake* mushrooms (Qiu et al., 2022). The values of a and b are 1.72 and −0.28, respectively, which is assumed similar to the values obtained for white button mushrooms (Paudel et al., 2015). Note that the irreversibility of denaturation implies that the interaction parameter retains the values according to the highest temperature experienced.

The effective water volume fraction $\tilde{\phi}_{w,eff}$ accounts for hydrogen bonding of all plasticizers present in the system, and it is defined as follows (van der Sman and Mauer, 2019):

$$\tilde{\phi}_{w,eff} = \phi_w + \sum_i \phi_{s,i}\left(\frac{N_{OH,S}\nu_w}{N_{OH,w}\nu_s}\right) \tag{11}$$

Here, ϕ_w and $\phi_{s,i}$ are the volume fraction of water and the solutes i, respectively. ν_w and ν_s are the molar volume of water and solutes, respectively. The $\frac{N_{OH,S}}{\nu_s}$ represents the number of H-bonding sites effectively available within the molar volume of solutes for intermolecular interactions. The values of N_{OH} for water, mannitol, and trehalose are 2, 3.56, and 7.72, respectively (van der Sman, 2016; van der Sman and Mauer, 2019).

Pitzer theory for $\mathbf{a}_{\mathrm{w,ion}}$.

Earlier for salted meat products, the Pitzer theory was combined with Flory Huggins Free Volume (FHFV) theory, based on the assumption of little interaction between salt and proteins (van der Sman, 2012). We take $a_{w,ionic}$ as the contribution from ash (phosphate, KH_2PO_4). In the Pitzer theory the state of electrolyte solutions is expressed in terms of the osmotic coefficient Φ:

$$(\Phi - 1) = -A_\Phi z_i^2 \frac{\sqrt{I}}{1 + b\sqrt{I}} + \left(\beta_{ij}^{(0)} + \beta_{ij}^{(1)}\ exp^{-\alpha\sqrt{I}}\right)m \tag{12}$$

with the relation between the osmotic coefficient and the water activity:

$$\mathbf{ln}\left(\mathbf{a}_{\mathrm{w,ion}}\right) = -\Phi * \mathbf{M}_{\mathrm{w}} \sum_{\mathrm{i}} m \tag{13}$$

$A_\Phi = 0.391$ is the Debye factor, $Z_i = 1$ is the valency of the salt, $\boldsymbol{\alpha} = 2$ and $\mathbf{b} = 1.2$ are constants as determined by Pitzer, β_{ij}^n are parameters, which are specific for ion pairs ij. For KH_2PO_4, $\beta^0_{KH_2PO_4} = -0.0678$ and $\beta^1_{KH_2PO_4} = -0.1042$ (Pitzer and Mayorga, 1973). $I = \frac{1}{2}\sum z_i^2 m_i$ is the ionic strength on molality basis, m is the molality of the electrolyte, which is the number of mole of solute per kg of water. $\mathbf{M}_{\mathrm{w}}$ is the molecular weight of water, 18 g/mol.

3.2. Viscoelastic relaxation model

A simple idealization of the viscoelastic characteristics of a material is the Maxwell model, which describes how mechanical stress changes with time:

$$\frac{d\sigma}{dt} = -\frac{\sigma}{\tau} + E_s\frac{d\varepsilon}{dt} \tag{14}$$

$\boldsymbol{\tau}$ is the viscoelastic relaxation time, $\boldsymbol{\varepsilon}$ is the total strain, and $\mathbf{E}_{\mathrm{s}}$ is the elastic (shear) modulus. $\boldsymbol{\sigma}$ is the stress.

During the viscoelastic relaxation phase of a compression test, the total strain is constant, i.e. $\frac{d\varepsilon}{dt} = 0$, and consequently, the stress relaxes via a single exponential function:

$$\sigma(t) = \sigma_0 \exp\left(-\frac{t}{\tau}\right) \quad (15)$$

$\sigma_0 = E_s\varepsilon_0$, ε_0 is the initial strain during the relaxation phase.

For complex materials like vegetables, a single relaxation time model is insufficient to describe their viscoelastic behaviour (Ozturk, Oguz K. and Takhar, Pawan S., 2019a). Hence, we have fitted the results of stress relaxation during the compression test with a stretched exponential model, also known as the Kohlraush–Slonimsky equation (Barua and Saha, 2016; Junisbekov et al., 2003).

$$\sigma(t) = (\sigma_0 - \sigma_\infty)\exp\left(-\frac{t}{\tau}\right)^{\beta} + \sigma_\infty \quad (16)$$

where σ_0 is the initial stress at the beginning of the stress relaxation phase; σ_∞ is the equilibrium modulus when t $\rightarrow\infty$; τ is the characteristic relaxation time. The stretched exponential model can be seen as the approximation of the fractional viscoelastic model (Simpson et al., 2013), which has been used for characterizing the viscoelastic properties of apples during drying (Mahiuddin et al., 2018). The applicability of fractional derivative models and stretched exponentials implies the existence of a broad distribution of relaxation times (Larson, 1985). Numerically, fractional derivative models are difficult to solve, therefore they are often approximated with a Prony series (Pettermann and Hüsing, 2012), which is similar to a generalized Maxwell model:

$$\sigma(t) = (\sigma_0 - \sigma_\infty)\exp\left(-\frac{t}{\tau}\right)^{\beta} + \sigma_\infty \approx \sum_{1}^{k}\sigma_i \exp\left(-\frac{t}{\tau_i}\right) + \sigma_\infty \quad (17)$$

4. Results and discussion

4.1. Sorption isotherms of powdered dried mushrooms

Fig. 1a shows moisture sorption isotherms of powdered mushrooms with different drying treatments, obtained from dual sorption-desorption cycle measurements. One can observe the hysteresis between the sorption and desorption branches of the first cycle isotherms (with their difference shown in Fig. 1b). The hysteresis phenomenon is also reported in previous studies for mushrooms (Argyropoulos et al., 2010; Pascual-Pineda et al., 2020). When mushroom samples were subjected to a second sorption-desorption cycle, we found that hysteresis was reduced for all drying treatments. Similarly (Keating et al., 2013), reported that hysteresis vanished in man-made hemicellulose (galactomannan) films above 75% RH at 25 °C and attributed it to the softening of the hemicelluloses at this humidity (Hill et al., 2012). found a significant decrease in the sorption hysteresis for wood during the second and third cycles. The given explanation for this hysteresis reduction is the relaxation of internal stresses during the adsorption branch of the first cycle (Hill et al., 2009, 2012; Kohler et al., 2003). These studies induced our assumption that MSIs of dried mushroom samples obtained from multiple sorption-desorption measurements present the real moisture sorption equilibrium. Moreover, all second-cycle MSIs of the samples with different drying treatments largely overlap, as shown in Fig. S1b. This makes us confident that all samples have reached a similar equilibrium, irrespective of their drying

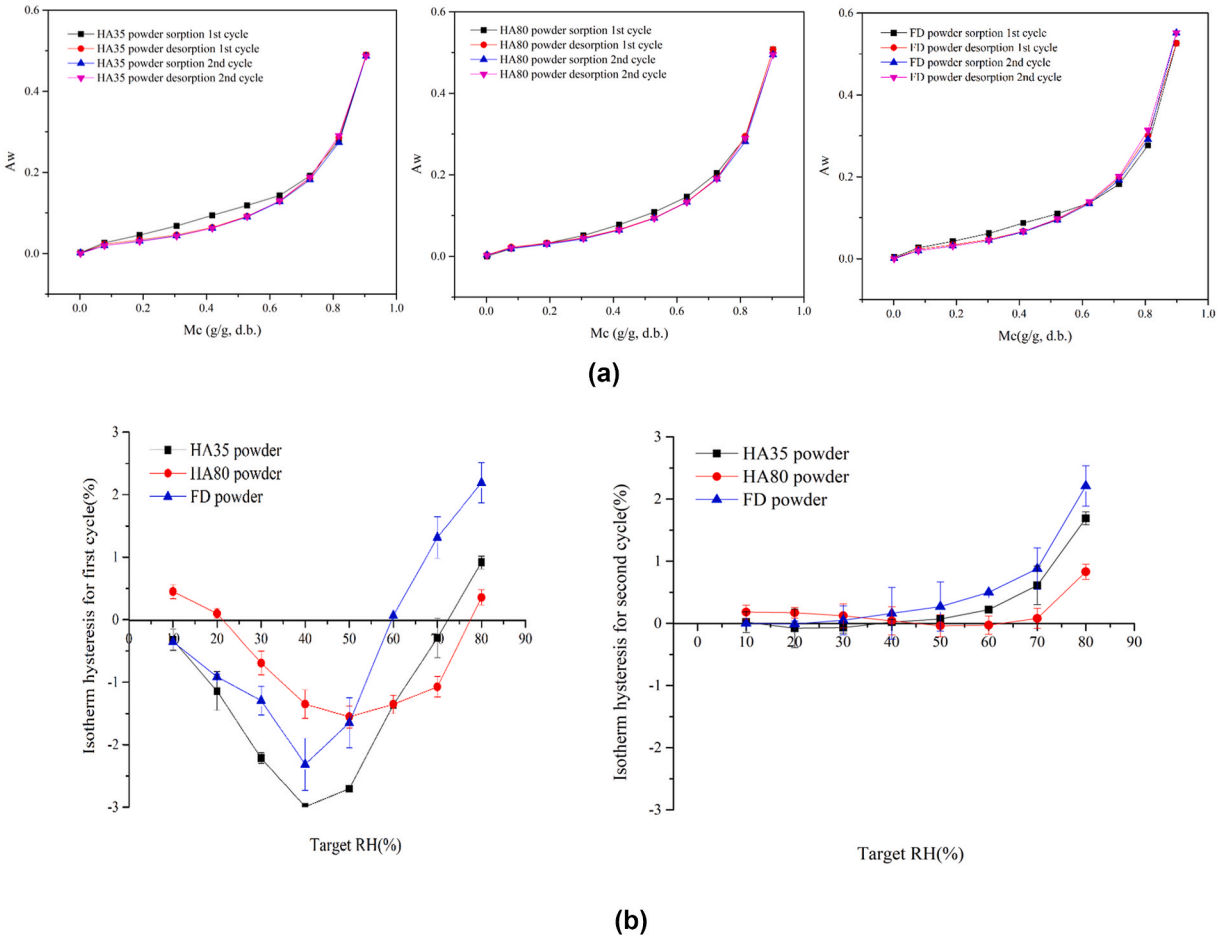

Fig. 1. MSIs (a) and hysteresis (b) for HA35, HA80, and FD dried *shiitake* mushroom powders (b left: first sorption-desorption cycle; b right: second sorption-desorption cycle).

pretreatments. We note in Fig. 1b right, there are still differences in the high water activity range. We assume these differences are not attributed to the hysteresis but to the water holding capacity (WHC) differences.

4.2. Effect of protein denaturation on MSI interpreted with Flory-Huggins theory

In this section, we analyze the effect of protein denaturation on moisture sorption isotherms on 1) the hysteresis observed during the first sorption-desorption cycle and 2) the hysteresis variation in the "equilibrium" MSI between treatments as observed during the second cycle. One of the starting hypotheses was that hysteresis might be caused by protein denaturation. From the observation of MSIs for HA80 samples, we observe hysteresis during the first sorption-desorption cycle, which is almost reduced to zero during the second sorption-desorption cycle. We note that protein denaturation happened only in HA80 and FD treatments (due to cold denaturation). Given the mild product temperatures during HA35 treatment one can safely assume that the proteins remain in the native state. Protein denaturation happening at high temperatures, as during HA80, is commonly assumed to be irreversible, i.e. the protein will not fold back to the native state. Concerning the FD we note that in literature, there is no consensus on whether cold denaturation is (ir)reversible (Lau et al., 2013). Hence, we know for certain that the proteins have not changed their state during the DVS experiments of HA35 and HA80 samples. Consequently, we cannot attribute the hysteresis reduction to the protein denaturation, as the protein remained denatured througout the DVS experiment.

Furthermore, we give an analysis based on the second-cycle MSIs of HA35 and HA80 dried samples. The protein denaturation degree can be quantified by the temperature-dependent interaction parameter between protein and water (van der Sman, 2012), based on FH theory. It is noted that after HA drying (T > 35 °C), the (partial) protein denaturation is irreversible (Baltacıoglu et al., 2015), implying that the interaction parameters between water and protein remain at the values of χ as imposed by the drying treatment. As depicted in Table 2, we calculated the interaction parameters ($\chi_{pro,w}$ and χ_{pro,w_1}) between protein and water according to Eq. (10), assuming that product temperature has reached drying temperature at the end of drying. We found that the interaction parameters increased promptly when the drying temperature was over 80 °C. Coincidentally, the protein denaturation temperature of *shiitake* mushrooms was measured to be as high as 76 °C (Qiu et al., 2021), meaning the interaction parameter can quantitively describe the denaturation degree. Variation of the interaction parameters for samples obtained from different drying temperatures indicates the protein denaturation is supposed to affect the moisture sorption. Then we applied the FH theory model to predict the MSIs obtained at 35 °C and 80 °C. The predicted MSIs are comparable to the experimental curves measured during the second sorption-desorption cycle. Thus, our calculations can accurately predict the equilibrium sorption isotherm (second cycle). However, a very limited difference is found between both predicted and measured MSIs of HA35 and HA80 dried samples, as shown in Fig. 2. Consequently, we tend to conclude that protein denaturation should not be the cause for hysteresis reduction but present some influence on the equilibrium moisture sorption of mushrooms.

Table 2
Calculated interaction parameters of protein for *shiitake* mushroom.

	35 °C	50 °C	65 °C	80 °C
χ_{pro,w_1}	0.800	0.800	0.809	1.103
$\chi_{pro,w}$	0.734	0.734	0.741	0.970

4.3. Effect of cell membrane integrity on MSI

4.3.1. Cell membrane integrity of mushrooms

The fate of cell membrane integrity due to the different drying methods of HA35, HA80, and FD was first investigated with transmission electron microscopy (TEM). Note, our dried samples were milled to powders to allow fast MSI measurements. As shown in Fig. 3, when taking the TEM images of fresh mushrooms as the reference, we found that HA35 dried powder samples retained intact cell membranes, while HA80 and FD dried ones present severe plasmolysis, cell membrane damage, and cell wall distortion. These results were consistent with our previous study (Qiu et al., 2021, 2022). Cell membrane rupture might be due to the denaturation of membrane proteins, or the (liquid crystal/gel) phase transition of membrane lipids (Lewicki and Pawlak, 2003, 2005; Voda et al., 2012). Besides, there is an interesting finding from the intact cell membrane of HA35 dried samples; namely, no damage happens on the cell membrane during milling.

4.3.2. Effect of cell membrane integrity on MSI interpreted with theory

As in the previous section, we first investigate the possible effect of cell membrane rupture on hysteresis. Likewise, cell membrane rupture is irreversible processes, happening at elevated temperatures (T > 45 °C) (Hu et al., 2021), or during freezing (Sman, 2020). Hence, we can follow a similar line of reasoning concerning its effect on hysteresis. For there is no change in the state of the cell membrane during the DVS measurements, the hysteresis reduction during the second sorption-desorption cycle cannot be attributed to the loss of cell membrane integrity.

To evaluate the effect of cell membrane integrity on the "equilibrium" moisture sorption isotherms, we compared theoretically calculated moisture sorption isotherms with experimental ones obtained from the second sorption-desorption cycle measurement. We assume all ingredients in the mushroom powder with ruptured membranes constitute a single, homogeneous mixed phase. While ingredients in the powder with intact membranes constitute a two-phase system, with solutes in the vacuole representing one phase, and the biopolymers existing in the cell wall and cytoplasm representing a second phase. The two-phase system is separated by the (vacuole) membrane, which allows the partitioning of water between phases until equilibrium is reached. Therefore, the HA35 dried sample having an intact cell membrane can be seen as a phase-separated system, while FD and HA80 dried samples presenting a ruptured cell membrane should be taken as a mixture system. Considering the more even distribution of ingredients in FD samples than that in HA80 ones (shown in Fig. 3), we compared the measured second cycle MSIs of HA35 and FD samples with the predicted ones based on two-phase system and mixed system model, as shown in Fig. 4. We observe little difference between the predictive MSIs of the two systems. Similarly, when the relative humidity is lower than 70% (a_w < 0.7), there is little difference in measured second-cycle MSIs between the HA35 and FD samples.

However, at high relative humidity (a_w > 0.7), the experimental data shows differences in water holding capacity (WHC) between HA35 and FD samples (shown in Fig. 1b right). This difference could be due to the variation in cell membrane integrity, in which intact cell membranes can restore the water holding in the vacuole and thus the turgor pressure via the stretching of the cell walls. Furthermore, we assume this stretching, which indicates elastic properties of samples, after the cell membrane restoration varies with different drying treatments. For example, during freeze-drying, cell walls are compacted firmly, leading to an increase in crosslink density and elasticity (Voda et al., 2012). Therefore, from the theoretical and experimental evaluation, we conclude that the state of cell membrane integrity mainly affects the moisture sorption of mushroom samples due to its contribution to water holding capacity.

4.4. Effect of mechanical stress relaxation on MSI

Mechanical stress within the matrix has been reported in studies

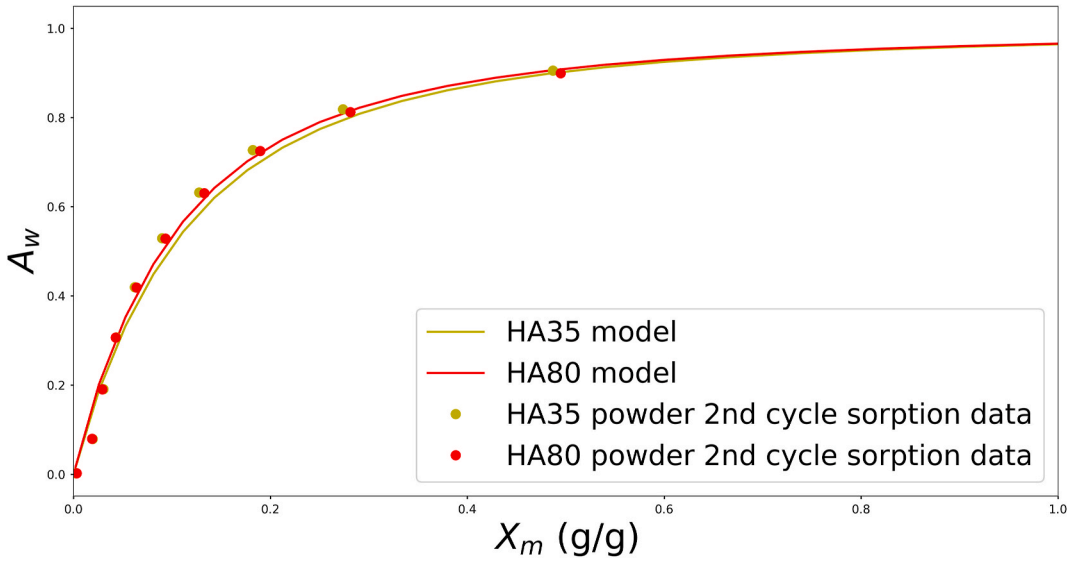

Fig. 2. Predictions and experimental data of sorption isotherms for HA35 and HA80 dried mushroom powders at 25 °C.

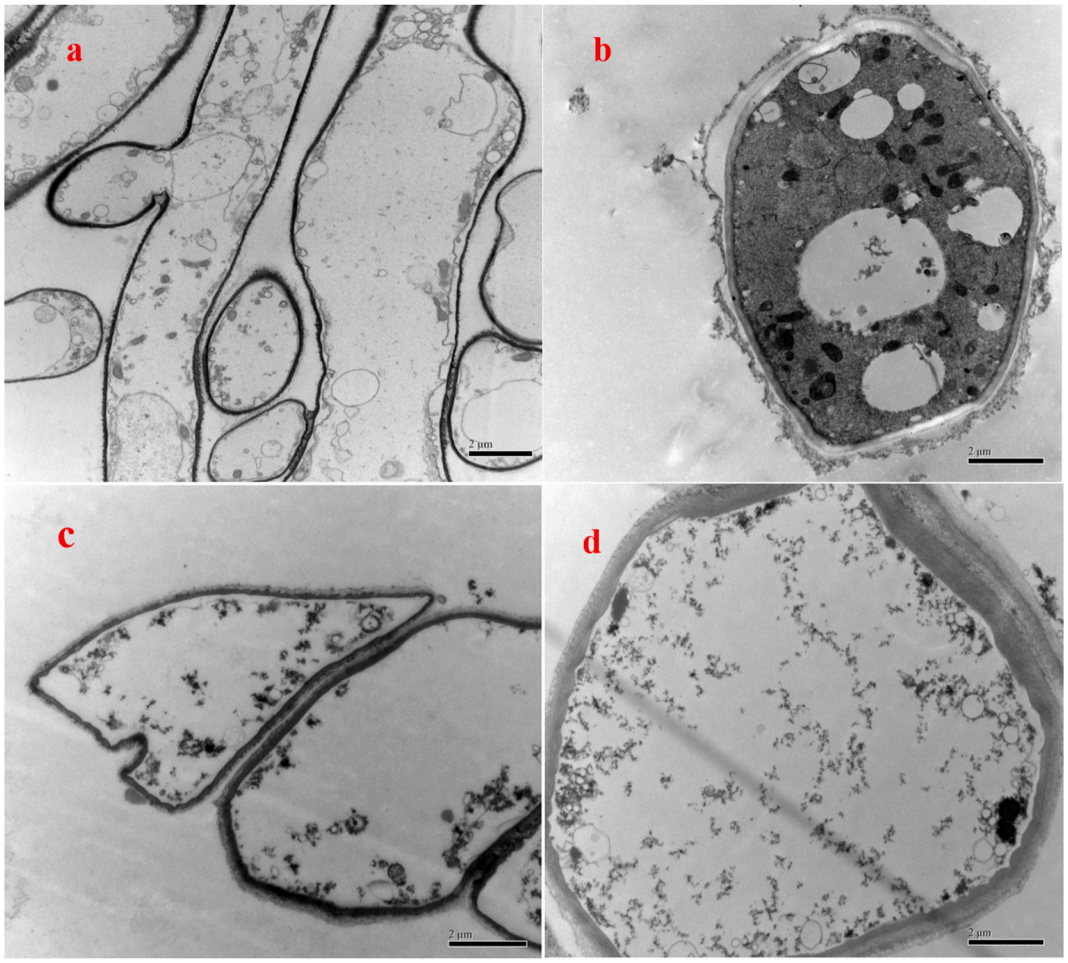

Fig. 3. TEM of mushroom samples (a: fresh mushroom; b: HA35 dried powder; c: HA80 dried powder; d: FD dried powder).

related to hydration (van der Sman et al., 2013b), and it is considered an important cause affecting the moisture sorption of samples at high water activities (Cornet et al., 2020; Hill et al., 2012; Paudel et al., 2015; Xie et al., 2011; Ying et al., 2013). (van der Sman et al., 2013b) presented the contributions from the elastic energy of the crosslinked network of cell wall materials to the hydration properties of carrots and mushrooms, which follows the Flory-Rehner theory. Other researchers pointed out that the viscoelastic properties could affect the moisture

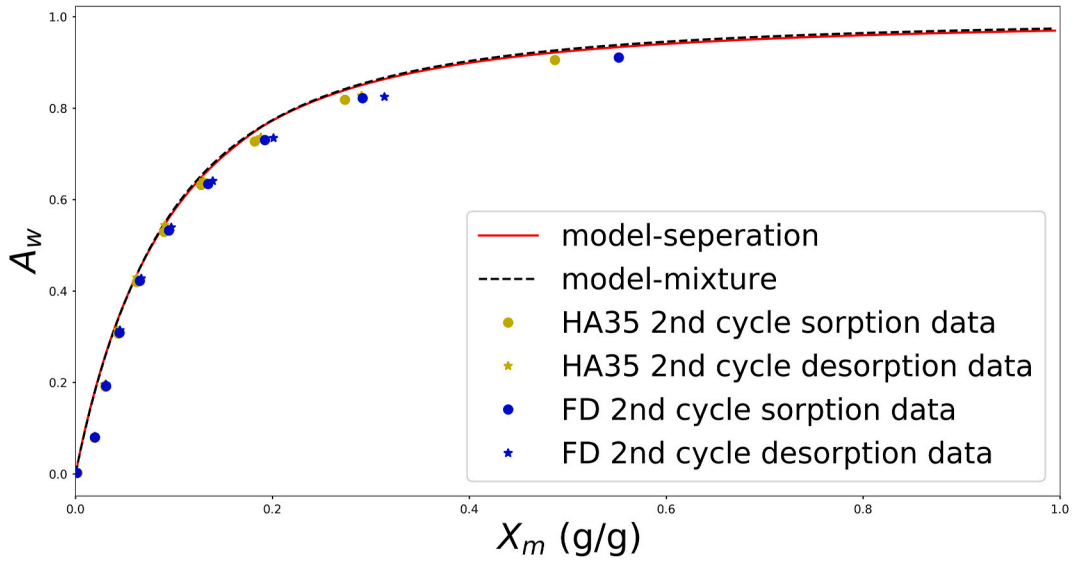

Fig. 4. Predictions and experimental data of sorption isotherms for HA35 and FD dried mushroom powders at 25 °C.

sorption via the stress relaxation (Champion et al., 2011; Hill and Xie, 2011; Oliver and Meinders, 2011; van der Sman and Meinders, 2011). Note that there can still be differences in moisture sorption if differences exist in pure elastic properties. Gels with different degrees of crosslinks will give a difference in moisture content at the same water activity, as described by Flory-Rehner theory. Therefore, the pure elastic properties should also be considered as equilibrium properties.

Many cellular food materials exhibit viscoelastic properties, such as strawberries, carrots, and apples, whose mechanical properties have been shown to be moisture and temperature-dependent (Mahiuddin et al., 2018; Ozturk, Oguz K. and Takhar, Pawan S., 2019a; Ozturk, Oguz Kaan and Takhar, Pawan Singh, 2019b). We note there is an interaction between water holding capacity, mechanical stress and cell membrane integrity. The cell wall can be considered a biopolymer network, and it provides structural rigidity under turgor conditions (Doulia et al., 2000; Veytsman and Cosgrove, 1998). At high a_w, solutes in the vacuole attract water, and the volume expansion stretches the cell wall, rendering the turgor pressure (Veytsman and Cosgrove, 1998). The high turgor pressure makes the cell wall stretch, rendering high tensile stress due to cellulosic fibers. A requirement for maintaining the turgor pressure is the integrity of the cell membrane, which inhibits solutes from diffusing out from the vacuole. When the cell membrane of samples remains intact after drying, the vacuole will grow after absorbing water (rehydration or sorption) and the turgor recovers, and the cell wall will be stretched again, resulting in the rebuilt-up of stress and structural integrity. However, suppose the cell membrane integrity is lost during drying, the solute will diffuse out of the vacuole during rehydration (Gekas et al., 1993), and the cell wall will not be stretched, thus without stress build up.

Hence, studying the viscoelastic properties of the cellular food matrix, which can also be caused by the cell membrane integrity change, provides valuable insights into its possible influence on MSI variations due to different processing histories.

4.4.1. *Overshoot during dynamic vapor sorption*

The occurrence of mechanical stress relaxation during moisture sorption of mushrooms is evident by the presence of overshoot in the dynamic responses, as measured by DVS (Oliver and Meinders, 2011). In Fig. 5 we use HA35 dried mushrooms as an example and display typical dynamic moisture sorption curves obtained by DVS. The curve shows the sample weight varies with the environmental RH as a function of time. During the first cycle of moisture sorption measurement, several samples exhibit overshoots, i.e. the sample weight shows an initial increase while decreasing at a later stage, as depicted with the subgraphs in Fig. 5a. Similarly (Oliver and Meinders, 2011), also observed overshoots during the moisture sorption of gluten and starch films. They attributed it to the viscoelastic relaxation of the biopolymers. However, during the second cycle of sorption-desorption, the overshoots and the hysteresis disappear (as shown in the subgraphs of Fig. 5b and in Fig. 1b). Also, for the mushrooms, we assume the overshoot (and hysteresis reduction) is due to the stress relaxation during each RH step. At the end of the first sorption cycle, $T > T_g$, the sample eventually completes the relaxation of the stresses, leading to the absence of overshoots during the second cycle. Below, we will show experimentally that mushrooms indeed exhibit viscoelastic properties, enabling stress relaxation.

4.4.2. *Viscoelastic properties of mushrooms with different moisture contents*

Since the viscoelastic property at the length scale of mushroom powder (micron scale) is hard to measure, we take a convenient way to measure the stress relaxation of mushroom powder via the compression and stress relaxation test on cylindrical mushroom samples. As shown in Fig. 6, we examined the viscoelastic properties of cylindrical mushroom samples with different moisture contents obtained during hot air drying at 35 °C and 80 °C. It shows that the stress-time curve mainly consists of two phases: compression and stress relaxation. During compression, all samples showed an increase in stress until the compression reached the expected strain. Subsequently, the stress gradually decreases over time in the relaxation phase, while holding the sample at the defined strain. This relaxation phase indicates the viscoelastic (stress relaxing) property of mushrooms.

In this study, we are mainly concerned about the initial and residual stress and the relaxation time (distribution) of cylindrical mushroom samples during the stress relaxation phase. It shows that all these parameters vary with moisture content. We observe decreasing initial stress in the range of moisture content (MC) larger than 0.91 g/g (d.b.) for HA35, and MC larger than 0.64 g/g (d.b.) for HA80. However, for

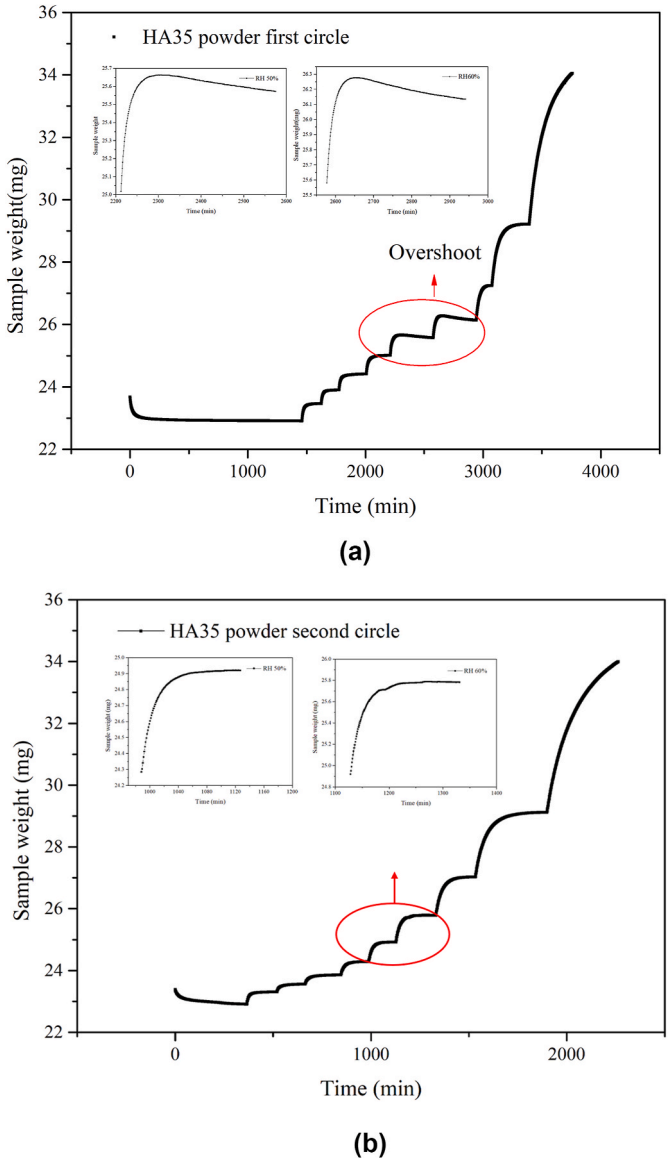

Fig. 5. The kinetic data obtained during the first (a) and second cycle (b) MSI measurements for HA35 dried mushroom powder.

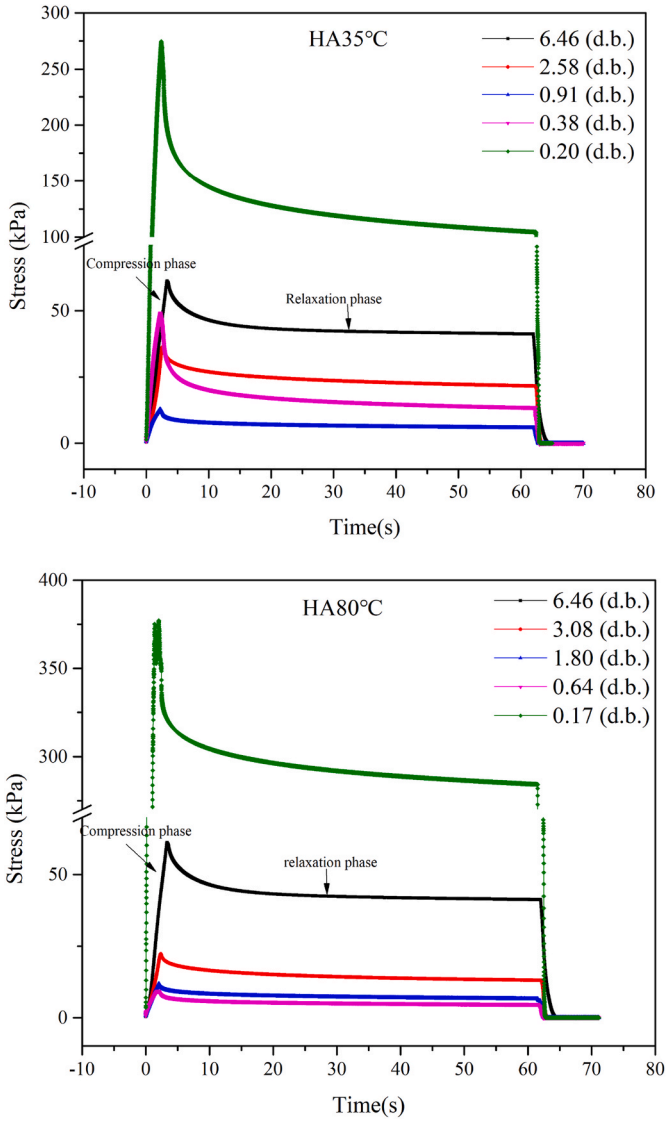

Fig. 6. Stress relaxation curves of cylindrical mushroom samples with different moisture contents during HA35 and HA80 drying.

smaller MC the initial stress increases again. A similar initial decrease of stress (relaxation modulus) was also found for apples, strawberries, and carrots using similar compression tests (Mahiuddin et al., 2018; Ozturk, Oguz K. and Takhar, Pawan S., 2019a; Ozturk, Oguz Kaan and Takhar, Pawan Singh, 2019b). Besides, it was also observed that the stress of carrots (relaxation modulus) increased again at low moisture contents. This range was not measured for strawberries or apples. The initial decrease of stress/relaxation modulus could be attributed to the turgor loss. The latter can be either due to the rupture of the cell membrane (as in the case of HA80), or the loss of stretching in the cell wall and possible plasmolysis (without rupture of the cell membrane, as in the case of HA35) (Prawiranto et al., 2018). This leads to the softening of the structure and the lowering of the stress levels (Ozturk, Oguz K. and Takhar, Pawan S., 2019a). However, when the moisture contents of mushrooms drop below 0.91 g/g (d.b.), the stress increases, which can be attributed to the loss of the plasticization action of water of the cell wall material, similar to those studies given by (Ozturk, Oguz K. and Takhar, Pawan S., 2019a).

4.4.3. *Stress relaxation effect on MSI interpreted with viscoelasticity*

The response of mushrooms in the stress relaxation phase cannot simply be described with a single relaxation-time Maxwell model, as evident by the long tailing of the stress relaxation. As indicated by the use of the fractional derivative model by (Mahiuddin et al., 2018), there is a distribution of relaxation times. A fractional derivative model can be approximated by the stretched relaxation model Eq. (17). A detailed exposition of fractional viscoelastic models can be referred to (Katicha and Flintsch, 2012; Mainardi and Spada, 2011). The fitting plots of stress-time curves during the relaxation phase fitted with the stretched exponential model are shown in Figs. S2–4. The values of σ_0 , τ, β, σ_∞ are given in Table 3, which were averaged from the fitting of stress-time curves with the stretched exponential model.

Table 3
Elastic modules and parameters obtained from the fitting curves at different moisture contents (drying at 35,80 °C).

Samples	Moisture content **Mc (d.b.)**	Initial stress σ_0 **(*kPa*)**	Relaxation time **τ (s)**	Power β	Residual stress σ_∞ **(*kPa*)**	Coefficient of determination R^2	Root Mean Square Error **RMSE**
Fresh	6.46 ±0.23	61.23 ±4.35^{cd}	3.36 ±0.048^{cd}	0.56 ±0.032^{a}	41.31 ±15.89^{c}	0.9987	0.1141
HA 35	2.58 ±0.32	36.17 ±0.3^{d}	12.5 ±0.0089^{f}	0.31 ±0.056^{b}	17.06 ±2.15^{d}	0.9988	0.08623
	0.91 ±0.14	12.86 ±2.43^{d}	2.17 ±0.061^{c}	0.25 ±0.0029^{b}	4.83 ±0.81^{e}	0.9928	0.07985
	0.38 ±0.031	49.17 ±6.59^{c}	0.78 ±0.051^{a}	0.3 ±0.001^{b}	12.52 ±1.12^{de}	0.9840	0.5430
	0.2 ±0.032	274.62 ±19.83^{a}	1.45 ±0.029^{c}	0.26 ±0.0037^{b}	86.19 ±7.42^{b}	0.9912	2.0578
HA 80	3.08 ±0.081	22.32 ±4.95^{d}	15.8 ±0.079^{f}	0.36 ±0.28 ^{ab}	10.47 ±3.42^{de}	0.9998	0.02072
	1.8 ±0.1	11.86 ±2.37^{d}	9.09 ±0.023^{ef}	0.25 ±0.053^{b}	4.79 ±1.00^{e}	0.9976	0.039
	0.64 ±0.04	9.35^{d} ±2.92^{d}	5.00 ±0.047^{de}	0.25 ±0.0071^{b}	3.6 ±0.37^{e}	0.9977	0.0310
	0.17 ±0.03	377.09 ±0.72^{b}	1.35 ±0.086^{b}	0.21 ±0.022^{b}	267.37 ±18.77^{a}	0.9843	1.31

Values are mean ± standard deviation, values in the same column followed by different superscript letters are significantly ($p < 0.05$) different.

The initial stress (σ_0) and residual stress (σ_∞) during the compression phase of samples treated by HA35 and HA80 present the same trend as illustrated in 4.4.2. According to (Rathinaraj et al., 2022), the value of fractional order (similar to β) of about 0.3 indicates a broad distribution of relaxation times, meaning that some fraction of the stress takes a very long time to relax, as indicated by the long tailing in the stress relaxation. The power (β) of stretched exponential for most samples is quite similar, although these samples show different moisture content. This is consistent with similar exponents of the fractional model from the study conducted by (Mahiuddin et al., 2018). In theory, one can expect that both powers are similar for different moisture contents and temperatures. The residual stresses σ_∞, which will not relax, remain to give an elastic contribution to the chemical potential.

There are two kinds of elastic contributions in the moisture sorption of food. The first case is when the food material is in a glassy state, it has become elastic, with a prolonged structural relaxation time. Hence, it behaves as an elastic solid. Traditionally, this elastic contribution is described by the Free Volume extension of the FH theory, but it might also be replaced by a description similar to Flory-Rehner. The Leibler-Sekimoto model is an example of such a model that takes the elastic contribution of the glassy state into account (Leibler and Sekimotot, 1993). The second case is when the food material consists of a cross-linked biopolymer network in the rubbery state. Its moisture sorption/water holding behaviour is described by the Flory-Rehner theory, which is another extension of the FH theory (van der Sman et al., 2013a). Flory -Rehner theory learns that elastic stresses need to be accounted for in the chemical potential of water (Gosline, 1978; van der Sman, 2012):

$$\Delta\boldsymbol{\mu}_{w\_poly} = \Delta\boldsymbol{\mu}_{w,mix} + \Delta\boldsymbol{\mu}_{w,elastic} = \nu_w(-\boldsymbol{\Pi}_{mix} + \boldsymbol{\Pi}_{elastic})$$

with ν_w the molar volume of water. The last term equals the elastic stress:

$$\boldsymbol{\Pi}_{elastic} = \boldsymbol{\sigma}$$

Initially, Flory-Rehner theory assumes a purely elastic material at large deformations. Mushrooms are viscoelastic materials as illustrated above, indicating the exist of elastic stress contribution to the moisture sorption. Hence, the above equation for the chemical potential of water still holds. However, based on the viscoelastic properties of mushrooms shown in study, we assume the stress relaxation effect on MSI should be coupled to the FH theory with a viscoelastic model, like the (generalized) Maxwell model that can describe the stress relaxation with time and has a distribution of relaxation times. The elastic modulus and relaxation time are, in general, temperature and moisture dependent as shown above. Furthermore, the generalized Maxwell model would need adaption to large deformations (van der Sman, 2015).

5. Conclusion

Different drying treatments (HA35, HA80, and FD) performed on mushrooms have led to different moisture sorption characteristics of dried mushroom powder, like the variation of hysteresis between the sorption and desorption branches of the isotherm. Hysteresis was reduced when the powdered dried mushroom samples were subjected to a second sorption-desorption cycle. Similar to (Oliver and Meinders, 2011), we pose that the hysteresis reduction is caused by the viscoelastic relaxation of the stress, that was built up during the drying treatments. We showed that neither protein denaturation nor cell membrane integrity significantly affect hysteresis. Retention of cell membrane integrity did influence the moisture sorption of dried mushroom samples in the high RH range, where it influences WHC. Furthermore, it helps restore turgor, and improved rehydration of mildly dried products, as shown in our previous study (Hu et al., 2021, 2022). Hence, retention of cell membrane integrity should be considered when designing drying systems for products aiming at high-volume recovery after rehydration. Severe drying conditions as HA80 lead to compacted cellular tissues, with high levels of stresses locked in after drying. The stress will relax away slowly, inhibiting restoration of initial microstructure during rehydration (Ho et al., 2013; Voda et al., 2012). For a quantitative description of drying processes, aimed at their design or optimization, one should incorporate the build-up of mechanical stresses due to the shrinkage of food materials during drying, their viscoelastic relaxation, and the inclusion of elastic stresses in driving forces of moisture sorption. This can be accomplished by modeling the stress via integration of the momentum balance, coupled to a viscoelastic constitutive model (generalized Maxwell) for the stress, and inclusion of this time-dependent stress in the Flory-Rehner theory, rendering the driving force for moisture transport (i.e. chemical potential of water).

Author statement

Hu Lina: Conceptualization, Investigation, Software, Writing- Original draft preparation. Bi Jinfeng:Supervision, Funding acquisition. Jin Xin: Supervision, Conceptualization, Methodology, Reviewing and Editing. Ruud van der Sman:Supervision, Conceptualization, Methodology, Reviewing and Editing.

Declaration of competing interest

The authors declare that they have known no competing financial interests or personal relationships that could have appeared to influence the work reported in this paper.

Data availability

Data will be made available on request.

Acknowledgments

This work was supported by the National Natural Science Foundation of China (32001719). We also thank WFBR (Wageningen Food Biobased Research) and the Internation Exchange Grant for Graduate Students of the Chinese Academy of Agricultural Sciences (2021) for providing funding for the stay of Lina Hu at Wageningen University & Research.

Appendix A. Supplementary data

Supplementary data to this article can be found online at https://doi.org/10.1016/j.jfoodeng.2023.111506.

References

Argyropoulos, D., Alex, R., Mueller, J., 2010. Establishing Moisture Sorption Isotherms of Wild Mushroom Varieties Using a Dynamic Vapor Sorption Method, XVIIth World Congress of the International Commission of Agricultural Engineering (CIGR)-Section VI: Postharvest Technology and Process Engineering, Quebec City, Canada, pp. 13–17.

Baltacıoglu, H., Bayındırlı, A., Severcan, M., Severcan, F., 2015. Effect of thermal treatment on secondary structure and conformational change of mushroom polyphenol oxidase (PPO) as food quality related enzyme: a FTIR study. Food Chem. 187, 263–269. https://doi.org/10.1016/j.foodchem.2015.04.097.

Barua, B., Saha, M.C., 2016. Incorporating density and temperature in the stretched exponential model for predicting stress relaxation behavior of polymer foams. J. Eng. Mater. Technol. 138 (1) https://doi.org/10.1115/1.4031426.

Burnett, D.J., Garcia, A.R., Thielmann, F., 2006. Measuring moisture sorption and diffusion kinetics on proton exchange membranes using a gravimetric vapor sorption apparatus. J. Power Sources 160, 426–430. https://doi.org/10.1016/j.jpowsour.2005.12.096.

Buwjoom, T., Tangtaweewipat, Suchon, Thongwittaya, N., Yamauchi, K.-e., 2004. Chemical composition, nutrient digestibility and metabolizable energy of shiitake mushroom stalk meal. J. Poultry Sci. 41, 322–328. https://doi.org/10.2141/jpsa.41.322.

Carneiro, A.A., Ferreira, I.C., Duenas, M., Barros, L., da Silva, R., Gomes, E., Santos-Buelga, C., 2013. Chemical composition and antioxidant activity of dried powder formulations of Agaricus blazei and Lentinus edodes. Food Chem. 138 (4), 2168–2173. https://doi.org/10.1016/j.foodchem.2012.12.036.

Caurie, M., 2007. Hysteresis phenomenon in foods. Int. J. Food Sci. Technol. (42), 45–49. https://doi.org/10.1111/j.1365-2621.2006.01203.x.

Champion, D., Loupiac, C., Simatos, D., Lillford, P., Cayot, P., 2011. Structural relaxation during drying and rehydration of food materials—the water effect and the origin of hysteresis. Food Biophys. 6, 160–169. https://doi.org/10.1007/s11483-011-9204-5.

Cornet, S.H.V., van der Goot, A.J., van der Sman, R.G.M., 2020. Effect of mechanical interaction on the hydration of mixed soy protein and gluten gels. Current Research in Food Science 3, 134–145. https://doi.org/10.1016/j.crfs.2020.03.007.

Doulia, D., Tzia, K., Gekas, V., 2000. A knowledge base for the apparent mass diffusion coefficient (DEFF) of foods. Int. J. Food Prop. 3 (1), 1–14. https://doi.org/10.1080/10942910009524613.

Dupas-Langlet, M., Dupas, J., Samain, S., Giardiello, M.-I., Meunier, V., Forny, L., 2016. A new method to determine “equilibrated” water activity and establish sorption isotherm by erasing surface history of the samples. J. Food Eng. 184, 53–62. https://doi.org/10.1016/j.jfoodeng.2016.03.023.

Fredriksson, M., Thybring, E.E., 2018. Scanning or desorption isotherms? Characterising sorption hysteresis of wood. Cellulose 25, 4477–4485. https://doi.org/10.1007/s10570-018-1898-9.

Gekas, V., Öste, R., Lamberg, I., 1993. Diffusion in heated potato tissues. J. Food Sci. 58, 827–831. https://doi.org/10.1111/j.1365-2621.1993.tb09368.x.

Gosline, J.M., 1978. The temperature-dependent swelling of elastin. Biopolymers 17, 697–707. https://doi.org/10.1002/bip.1978.360170312.

Hayat, M.A., 2012. Basic Techniques for Transmission Electron Microscopy. Academic Press, Elsevier, Netherlands.

Hill, C.A.S., Keating, B., Rautkari, L., Ramsay, J., Laine, K., Hughes, M., Constant, B., 2012. The water vapour sorption properties of thermally modified and densified wood. J. Mater. Sci. 47, 3191–3197. https://doi.org/10.1007/s10853-011-6154-8.

Hill, C.A.S., Norton, A., Newman, G., 2009. The water vapor sorption behavior of natural fibers. Journal ofApplied Polymer Science 112, 1524–1537. https://doi.org/10.1002/app.29725.

Hill, C.A.S., Xie, Y., 2011. The dynamic water vapour sorption properties of natural fibres and viscoelastic behaviour of the cell wall: is there a link between sorption kinetics and hysteresis? J. Mater. Sci. 46, 3738–3748. https://doi.org/10.1007/s10853-011-5286-1.

Ho, Q.T., Carmeliet, J., Datta, A.K., Defraeye, T., Delele, M.A., Herremans, E., Opara, L., Ramon, H., Tijskens, E., van der Sman, R., Van Liedekerke, P., Verboven, P., Nicolaï, B.M., 2013. Multiscale modeling in food engineering. J. Food Eng. 114 (3), 279–291. https://doi.org/10.1016/j.jfoodeng.2012.08.019.

Hu, L., Bi, J., Jin, X., Qiu, Y., van der Sman, R.G.M., 2021. Study on the rehydration quality improvement of shiitake mushroom by combined drying methods. Foods 10, 769. https://doi.org/10.3390/foods10040769.

Hu, L., Bi, J., Jin, X., Sman, R.v.d., 2022. Microstructure evolution affecting the rehydration of dried mushrooms during instant controlled pressure drop combined hot air drying (DIC-HA). Innovat. Food Sci. Emerg. Technol. 79, 103056 https://doi.org/10.1016/j.ifset.2022.103056.

Iiyama, K., Stone, B.A., Macauley, B.J., 1996. Changes in the concentration of soluble anions in compost during composting and mushroom (Agaricus bisporus) growth. J. Sci. Food Agric. 72, 243–249.

Jin, X., van der Sman, R.G.M., van Maanen, J.F.C., van Deventer, H.C., van Straten, G., Boom, R.M., van Boxtel, A.J.B., 2014. Moisture sorption isotherms of broccoli interpreted with the Flory-Huggins Free Volume theory. Food Biophys. 9 (1), 1–9. https://doi.org/10.1007/s11483-013-9311-6.

Julita Reguła, M.S., 2007. Dried shiitake (Lentinulla edodes) and oyster (Pleurotus ostreatus) mushrooms as a good source of nutrient. Acta Scientiarum Polonorum Technologia Alimentaria 6 (4), 135–142.

Junisbekov, T.M., Kestelman, V.N., Malinin, N.I., 2003. Stress Relaxation in Viscoelastic Materials. Science Publishers, Enfield, NH.

Katicha, S.W., Flintsch, G.W., 2012. Fractional viscoelastic models: master curve construction, interconversion, and numerical approximation. Rheol. Acta 51, 675–689. https://doi.org/10.1007/s00397-012-0625-y.

Keating, B.A., Hill, C.A.S., Sun, D., English, R., Davies, P., McCue, C., 2013. The water vapor sorption behavior of a galactomannan cellulose nanocomposite film analyzed using parallel exponential kinetics and the Kelvin–Voigt viscoelastic model. J. Appl. Polym. Sci. 129 (4), 2352–2359. https://doi.org/10.1002/app.39132.

Kohler, R., Dück, R., Ausperger, B., Alex, R., 2003. A numeric model for the kinetics of water vapor sorption on cellulosic reinforcement fibers. Compos. Interfac. 10 (2–3), 255–276. https://doi.org/10.1163/156855403765826900.

Larson, R.G., 1985. Constitutive relationships for polymeric materials with power-law distributions of relaxation times. Rheol. Acta 24, 327–334. https://doi.org/10.1007/BF01333961.

Lau, C.-C., Abdullah, N., Aminudin, N., Shuib, A.S., 2013. Effect of freeze-drying process on the property of angiotensin I-converting enzyme inhibitory peptides in grey oyster mushrooms. Dry. Technol. 31 (13–14), 1693–1700. https://doi.org/10.1080/07373937.2013.779584.

Lee, J.H., Lee, M.J., 2008. Effect of drying method on the moisture sorption isotherms for Inonotus obliquus mushroom. LWT - Food Sci. Technol. (Lebensmittel-Wissenschaft -Technol.) 41 (8), 1478–1484. https://doi.org/10.1016/j.lwt.2007.08.016.

Leibler, L., Sekimotot, K., 1993. On the sorption of gases and liquids in glassy polymers. Macromolecules 26 (25), 6937–6939.

Lewicki, P.P., Pawlak, G., 2003. Effect of drying on microstructure of plant tissue. Dry. Technol. 21 (4), 657–683. https://doi.org/10.1081/drt-120019057.

Lewicki, P.P., Pawlak, G., 2005. Effect of mode of drying on microstructure of potato. Dry. Technol. 23 (4), 847–869. https://doi.org/10.1081/DRT-200054233.

Mahiuddin, M., Khan, M.I.H., Duc Pham, N., Karim, M.A., 2018. Development of fractional viscoelastic model for characterizing viscoelastic properties of food material during drying. Food Biosci. 23, 45–53. https://doi.org/10.1016/j.fbio.2018.03.002.

Mainardi, F., Spada, G., 2011. Creep, relaxation and viscosity properties for basic fractional models in rheology. Eur. Phys. J. Spec. Top. 193, 133–160. https://doi.org/10.1140/epjst/e2011-01387-1.

Myhan, R., Markowski, M., Daszkiewicz, T., Zapotoczny, P., Sadowski, P., 2015. Non-linear stress relaxation model as a tool for evaluating the viscoelastic properties of meat products. J. Food Eng. 146, 107–115. https://doi.org/10.1016/j.jfoodeng.2014.09.006.

Oliver, L., Meinders, M.B.J., 2011. Dynamic water vapour sorption in gluten and starch films. J. Cereal. Sci. 54, 409–416. https://doi.org/10.1016/j.jcs.2011.08.005.

Ozturk, O.K., Takhar, P.S., 2019a. Physical and viscoelastic properties of carrots during drying. J. Texture Stud. 51, 532–541. https://doi.org/10.1111/jtxs.12496.

Ozturk, O.K., Takhar, P.S., 2019b. Selected physical and viscoelastic properties of strawberries as a function of heated-air drying conditions. Dry. Technol. 37 (14), 1833–1843. https://doi.org/10.1080/07373937.2018.1543701.

Pascual-Pineda, L.A., Hernández-Marañon, A., Castillo-Morales, M., Uzárraga-Salazar, R., Rascón-Díaz, M.P., Flores-Andrade, E., 2020. Effect of water activity on the stability of freeze-dried oyster mushroom (Pleurotus ostreatus) powder. Dry. Technol. 1–14. https://doi.org/10.1080/07373937.2020.1739064.

Patera, A., Derluyn, H., Derome, D., Carmeliet, J., 2016. Influence of sorption hysteresis on moisture transport in wood. Wood Sci. Technol. 50, 259–283. https://doi.org/10.1007/s00226-015-0786-9.

Paudel, E., Boom, R.M., van der Sman, R.G.M., 2015. Change in water-holding capacity in mushroom with temperature analyzed by Flory-Rehner theory. Food Bioprocess Technol. 8 (5), 960–970. https://doi.org/10.1007/s11947-014-1459-7.

Pedro, M.A.M., Telis-Romero, J., Telis, V.R.N., 2010. Effect of drying method on the adsorption isotherms and isosteric heat of passion fruit pulp powder. Food Sci. Technol. 30 (4), 993–1000.

Pettermann, H.E., Hüsing, J., 2012. Modeling and simulation of relaxation in viscoelastic open cell materials and structures. Int. J. Solid Struct. 49 (19–20), 2848–2853. https://doi.org/10.1016/j.ijsolstr.2012.04.027.

Pitzer, K.S., Mayorga, G., 1973. Thermodynamics of electrolytes. II. Activity and osmotic coefficients for strong electrolytes with one or both Ions univalent. J. Phys. Chem. 77 (19), 2300–2308. https://doi.org/10.1021/j100638a009.

Prawiranto, K., Defraeye, T., Derome, D., Verboven, P., Nicolai, B., Carmeliet, J., 2018. New insights into the apple fruit dehydration process at the cellular scale by 3D continuum modeling. J. Food Eng. 239, 52–63. https://doi.org/10.1016/j.jfoodeng.2018.06.023.

Qiu, Y., Bi, J., Jin, X., Hu, L., Lyu, J., Wu, X., 2021. An understanding of the changes in water holding capacity of rehydrated shiitake mushroom (Lentinula edodes) from cell wall, cell membrane and protein. Food Chem. 351, 129230 https://doi.org/10.1016/j.foodchem.2021.129230.

Qiu, Y., Bi, J., Jin, X., Wu, X., Hu, L., Chen, L., 2022. Investigation on the rehydration mechanism of freeze-dried and hot-air dried shiitake mushrooms from pores and cell wall fibrous material. Food Chem. 383, 132360 https://doi.org/10.2141/jpsa.41.322.

Rathinaraj, J.D.J., Keshavarz, B., FRS, G.H.M., 2022. Why the Cox-Merz Rule and Gleissle Mirror Relation Work: A Quantitative Analysis Using the Fractional K-BKZ Model.

Reis, F.S., Barros, L., Martins, A., Ferreira, I.C., 2012. Chemical composition and nutritional value of the most widely appreciated cultivated mushrooms: an inter-species comparative study. Food Chem. Toxicol. 50 (2), 191–197. https://doi.org/10.1016/j.fct.2011.10.056.

Salmén, L., Larsson, P.A., 2018. On the origin of sorption hysteresis in cellulosic materials. Carbohydr. Polym. 182, 15–20. https://doi.org/10.1016/j.carbpol.2017.11.005.

Simpson, R., Ramirez, C., Jaques, A., Nuñez, H., Almonacid, A., 2013. Fractional calculus as a mathematical tool to improve the modeling of mass transfer phenomena in food processing. Food Eng. Rev. 5, 45–55. https://doi.org/10.1007/s12393-012-9059-7.

Sman, R.G.M.v.d., 2020. Impact of processing factors on quality of frozen vegetables and fruits. Food Eng. Rev. 12, 399–420. https://doi.org/10.1007/s12393-020-09216-1.

van der Sman, R.G., 2015. Hyperelastic models for hydration of cellular tissue. Soft Matter 11 (38), 7579–7591. https://doi.org/10.1039/c5sm01032b.

van der Sman, R.G.M., 2012. Thermodynamics of meat proteins. Food Hydrocolloids 27 (2), 529–535. https://doi.org/10.1016/j.foodhyd.2011.08.016.

van der Sman, R.G.M., 2016. Sugar and polyol solutions as effective solvent for biopolymers. Food Hydrocolloids 56, 144–149. https://doi.org/10.1016/j.foodhyd.2015.12.001.

van der Sman, R.G.M., Jin, X., Meinders, M.B.J., 2013a. A paradigm shift in drying of food materials via Free-Volume concepts. Dry. Technol. 31 (15), 1817–1825. https://doi.org/10.1080/07373937.2013.829089.

van der Sman, R.G.M., Mauer, L.J., 2019. Starch gelatinization temperature in sugar and polyol solutions explained by hydrogen bond density. Food Hydrocolloids 94, 371–380. https://doi.org/10.1016/j.foodhyd.2019.03.034.

van der Sman, R.G.M., Meinders, M.B.J., 2011. Prediction of the state diagram of starchwater mixtures using the Flory–Huggins free volume theory. Soft Matter 7 (2), 429–442. https://doi.org/10.1039/c0sm00280a.

van der Sman, R.G.M., Paudel, E., Voda, A., Khalloufi, S., 2013b. Hydration properties of vegetable foods explained by Flory–Rehner theory. Food Res. Int. 54 (1), 804–811. https://doi.org/10.1016/j.foodres.2013.08.032.

Veytsman, B.A., Cosgrove, D.J., 1998. A model of cell wall expansion based on thermodynamics of polymer networks. Biophys. J. 75, 2240–2250. https://doi.org/10.1016/S0006-3495(98)77668-4.

Voda, A., Homan, N., Witek, M., Duijster, A., van Dalen, G., van der Sman, R., Nijsse, J., van Vliet, L., Van As, H., van Duynhoven, J., 2012. The impact of freeze-drying on microstructure and rehydration properties of carrot. Food Res. Int. 49 (2), 687–693. https://doi.org/10.1016/j.foodres.2012.08.019.

Xie, Y., Hill, C.A.S., Jalaludin, Z., Sun, D., 2011. The dynamic water vapour sorption behaviour of natural fibres and kinetic analysis using the parallel exponential kinetics model. Cellulose 18, 517–530. https://doi.org/10.1007/s10570-011-9512-4.

Ying, R., Rondeau-Mouro, C., Barron, C., Mabille, F., Perronnet, A., Saulnier, L., 2013. Hydration and mechanical properties of arabinoxylans and β-D-glucans films. Carbohydr. Polym. 96, 31–38. https://doi.org/10.1016/j.carbpol.2013.03.090.

Zhao, J.-H., Ding, Y., Nie, Y., Xiao, H.-W., Zhang, Y., Zhu, Z., Tang, X.-M., 2016. Glass transition and state diagram for freeze-dried Lentinus edodes mushroom. Thermochim. Acta 637, 82–89. https://doi.org/10.1016/j.tca.2016.06.001.